THE JOURNAL OF PHYSICAL CHEMISTRY Letters

Letter

pubs.acs.org/JPCL

Multiscale Theoretical Modeling of Plasmonic Sensing of Hydrogen Uptake in Palladium Nanodisks

M. Ameen Poyli,[†,‡] V. M. Silkin,[‡,¶,§] I. P. Chernov,[∥] P. M. Echenique,[†,‡,¶] R. Díez Muiño,[†,‡] and J. Aizpurua*[,†,‡]

[†]Centro de Física de Materiales CFM (CSIC-UPV/EHU), Paseo Manuel de Lardizabal 5, 20018 San Sebastián, Spain

[‡]Donostia International Physics Center (DIPC), Paseo Manuel de Lardizabal 4, 20018 San Sebastián, Spain

[¶]Departamento de Física de Materiales, Facultad de Químicas UPV/EHU, Apartado 1072, 20080 San Sebastián, Spain

[§]IKERBASQUE, Basque Foundation for Science, 48011 Bilbao, Spain

[∥]Tomsk Polytechnical University, pr. Lenina 30, 634050 Tomsk, Russia

ABSTRACT: We study theoretically the optical properties of palladium nanodisks during hydrogen uptake. A combination of an ab initio quantum mechanical description of the Pd−H dielectric properties and a full electrodynamical study of light scattering in the H-modified Pd nanodisks allows us to trace the shift of the localized surface plasmon as a function of the H concentration in the Pd−H disk. We follow the evolution of the plasmon peak energy for different admixtures of the Pd−H α and β phases and interpret quantitatively the experimental sensitivity of the plasmon energy shift to the structural inhomogeneity upon H absorption. Our multiscale theoretical framework provides a solid background for plasmonic sensing of structural domains, as well as for identifying H saturation conditions in metal hydride systems.

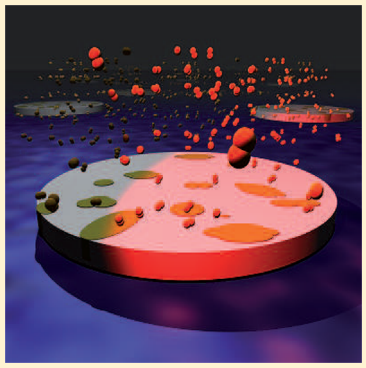

SECTION: Plasmonics, Optical Materials, and Hard Matter

Localized surface plasmon resonances (LSPRs) are collective excitations of conduction electrons in finite metallic structures. In nanometer-size systems, LSPRs appear at well-defined energies that depend on size and shape, as well as on the material itself.[1,2] The resonance energy can be also very sensitive to the external environment, making LSPRs a phenomenon extremely attractive for biological and chemical sensing. Standard sensing schemes are usually based on the LSPR shift produced when the nanoparticles are embedded in a given chemical environment.[3] With the help of plasmon-based strong local-field enhancements, sensing of very small amounts of H_2 has been recently achieved.[4] Chemical modifications within a nanosystem can also be monitored in real time through shifts in the LSPR position.[5−7]

A quite different and promising outlook in the context of plasmon-sensing is the possibility to oversee the change not only in chemical but also in physical properties, such as structural parameters.[5] Direct nanoplasmonic sensing has proven to be remarkably successful, for instance, in the study of hydrogen absorption by Pd nanoparticles.[5,6,8,9] Adsorption, absorption, and diffusion of H in Pd systems are processes of major importance in a variety of technologically relevant applications. In nanocatalysis for instance, subsurface H atoms substantially increase the efficiency of Pd nanoparticles in the hydrogenation of organic molecules.[10] Perfect absorption of visible radiation by Pd nanostructures has been recently explored in the design of novel H_2 sensors.[11] In fuel applications, metal hydrides are also recognized as an efficient and safe means for H storage in solid form.[12−15] Because better absorption and desorption kinetics of metallic nanoparticles offer faster storage and release of hydrogen,[16−19] real time plasmonic sensing of the absorption and desorption of hydrogen in Pd nanoparticles becomes a unique tool to obtain understanding of the metal hydride formation process and to improve the capabilities of existing hydrogen storage and sensing devices.

An accurate interpretation of the experimental trace of hydrogen uptake in Pd requires a theoretical framework that accounts for the changes in the optical properties of the material as it is structurally modified by the progressive presence of H. The description of the optical properties of the H−Pd system is not a simple task due to (i) the presence of different phases that H can adopt when absorbed in Pd (α and β phases) and (ii) the different length scales involved in the hydrogen uptake process requiring a multiscale approach, that is, an accurate description of the quantum mechanical effects associated with structural changes at the atomic scale together with a detailed description of the nanoscale where size, shape,

Received: June 15, 2012
Accepted: August 24, 2012

   dx.doi.org/10.1021/jz3007723 | *J. Phys. Chem. Lett.* 2012, 3, 2556−2561

and the environment affect the optical response of the whole mesoscopic system.

Here, we provide a theoretical framework to address the optical response of the mixed-phase hydrogen uptake in Pd nanodisks where we combine two different state-of-the-art methodologies to tackle both the atomic-scale structure of Pd−H and the mesoscopic-scale response of the Pd−H disk. Furthermore, an appropriate effective medium dielectric response to address the mixed-phase nature of the hydrogen uptake is also considered. To address the atomic-scale effect of the H difussion in Pd, we employ the dielectric function of different Pd−H stoichiometric mixtures obtained by means of ab initio calculations based on time-dependent density functional theory (TDDFT).[20,21] In a second step, classical electrodynamical calculations of the optical response of the Pd−H nanodisks are performed using the boundary element method (BEM)[22] to account for size, shape, and environment effects. Finally, to account for the double phase of the Pd−H system, we adopt a dielectric response based on a Bruggeman's effective medium that goes beyond the simple averaged response of the α (pure Pd domain) and β (Pd−H domain) phases. Comparing our results with recent experimental measurements of LSPR shifts in hydrogenized Pd nanosystems,[23] we identify the structural parameters that better adjust to the spectroscopic output. We thus show that LSPR sensing is not only an excellent tool to monitor H content in metal nanosystems but also a promising candidate to quantitatively determine structural changes and domain distributions in dynamical process.

A sensitive benchmark in the theoretical description of hydrogen uptake in Pd is the evolution of the plasmon peak energy when H is absorbed. Ab initio TDDFT-based calculations[24] of the dielectric optical response of bulk stoichiometric homogeneous PdH_x, for different x = H/Pd ratios showing a homogeneous distribution of H atoms in the lattice, are shown in Figure 1b. These calculations show that the bulk plasmon energy ω_P of PdH_x shifts to lower energies almost linearly[6,24] with H concentration x, from 7.78 eV in pure Pd to 4.25 eV in PdH.[20] The unit cells of the crystal lattices of pure Pd ($PdH_{x=0}$) and of Pd with H showing a 1:1 stoichiometry ($PdH_{x=1}$) used in these ab initio calculations are illustrated in Figure 1a. Absorption of H by a metal causes expansion of the lattice[25−27] and a change in the dielectric response.[28] The lattice parameters for each PdH_x system with different H concentration x have been obtained from total energy calculations, and the values have been found to be close to experimental data.[29] On the other hand, the internal relaxation of the Pd atoms around H atom positions[30] for ratios $x \neq 1$ can be neglected because of the weak influence of this effect on the optical properties.

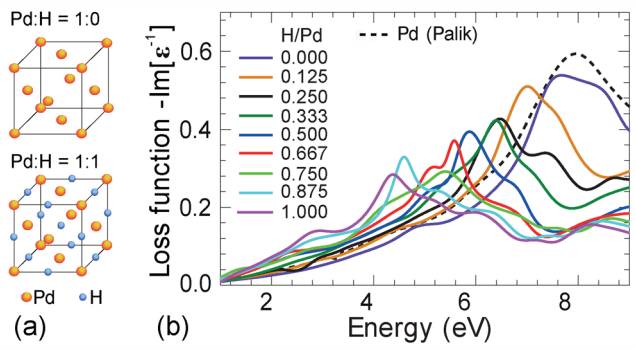

Figure 1. (a) Crystal lattice of pure Pd and fully hydrogenated Pd used in the ab initio calculations. H atoms occupy the octahedral interstitial sites in the face-centered cubic lattice of palladium to form PdH. (b) Dielectric loss function, $-\mathrm{Im}\{1/\varepsilon\}$, for bulk PdH_x obtained from ab initio TDDFT calculations and plotted for different H/Pd concentration values. For pure Pd, the calculated loss function (blue line) agrees with that obtained in energy loss[32,38−40] and optical[41,42] experiments and other ab initio calculations.[43−46] The black dashed line shows the data obtained from the optical measurements.[42]

In Pd nanostructures, a linear shift of the LSPR peak energy with increasing H concentration has also been measured, although the energy range is quite different from that in bulk.[6] To account for this difference, we proceed to perform full electrodynamical calculation of the extinction cross section for PdH_x disks by solving Maxwell's equations, in which we plug in the ab initio bulk dielectric function and the appropriate boundary conditions. To illustrate the profound effects that the morphological aspect of the PdH_x disks as well as the dielectric environment produce on the plasmonic response of the stoichiometric PdH_x systems, we first show in Figure 2a the resonance energy for different geometries of mesoscopic PdH_x structures as a function of H concentration x. We display the plasmonic resonance energies of PdH_x systems for (i) the bulk, (ii) the surface, and (iii) the dipolar LSPR in a spherical particle in the electrostatic limit when using the corresponding ab initio bulk dielectric functions. The bulk plasmon energy is obtained from the position of the peak in the loss function (Figure 1b). As mentioned before, the bulk plasmon energy of PdH_x linearly shifts with x but always remains in the UV range, even for a fully hydrogenated $PdH_{x=1}$ stoichiometry. The surface response of the vacuum−PdH_x interface is determined by the surface response function defined as $\mathrm{Im}\{(\varepsilon_{PdH_x} - 1)/(\varepsilon_{PdH_x} + 1)\}$, where ε_{PdH_x} is the dielectric function of PdH_x for different amounts of H, which presents a pole when $\varepsilon_{PdH_x} + 1 = 0$. The energy position of this pole evaluated with the ab initio dielectric function ε_{PdH_x} in Figure 1b is displayed as green squares in Figure 2a. The energies of these surface plasmons are slightly shifted to the red compared with the bulk resonances, with a quite constant shift for all H concentrations (slightly less than about 1 eV). Hence, the surface plasmon energies of all H concentrations are also in the UV. The dipolar plasmon position of the metallic nanoparticle given by $\mathrm{Im}\{(\varepsilon_{PdH_x} - 1)/(\varepsilon_{PdH_x} + 2)\}$ presents the resonance for $\varepsilon_{PdH_x} + 2 = 0$. These solutions are displayed in Figure 2a as blue squares. An additional shift is found in this case, bringing energies of the LSPR to a range between 6 eV for the pure Pd spherical particle and 2.5 eV for a sphere with an equal number of H and Pd atoms ($PdH_{x=1}$).

We also perform full electrodynamical calculations of the extinction cross section of isolated PdH_x disks as a function of the H/Pd ratio. The use of Pd disks is an effective way to lower the energy of the LSPR in the particles due to the coupling of the top and bottom surfaces of the disk that produces an extra red shift in the optical response.[31] The red shift resulting from the intraparticle coupling in the disks brings the LSPR energy to the visible region for a 20 nm thick disk of diameter 190 nm. For an isolated disk, the LSPR runs from 2.2 eV for pure Pd to 1.6 eV for $PdH_{x=1}$, represented by black squares in Figure 2a. Additionally, the deposition of the disk on a substrate causes a further reduction in the LSPR energy. The LSPR position is

dx.doi.org/10.1021/jz3007723 | J. Phys. Chem. Lett. 2012, 3, 2556−2561

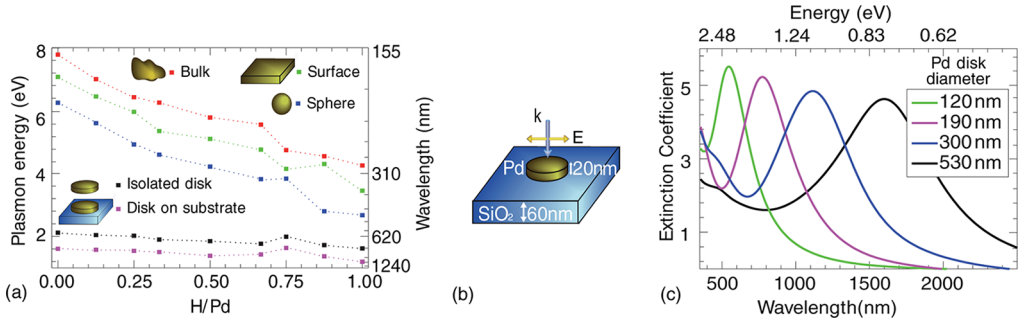

Figure 2. (a) Plasmonic resonance energies of the PdH_x systems for (i) bulk, (ii) surface, and (iii) dipolar LSPR in a spherical particle in the electrostatic limit, (iv) an isolated disk that is 20 nm thick and 190 nm in diameter, and (v) the same disk deposited on a SiO_2 substrate, obtained with use of dielectric functions calculated through the TDDFT as a function of the x = H/Pd ratio. The dotted lines are guides to the eye. (b) Schematics of the system used in the BEM calculations to obtain the far-field optical response of the PdH_x nanodisks. Disks of thickness 20 nm and different diameters are deposited on a 60 nm thick SiO_2 substrate and illuminated by a polarized plane wave incident normally from the top. (c) Extinction spectra calculated using the ab initio dielectric function for Pd disks of 20 nm thickness for different diameters.

represented in this case as pink squares in Figure 2a, showing that the interaction with the substrate causes a reduction in the LSPR energy of the disk by approximately 0.5 eV for all H concentrations. The LSPR position can be further tuned by varying the size of the disk. To reveal this, we implement electrodynamical calculations for pure Pd disks supported on SiO_2 (Figure 2b) as a function of disk size. This outlines the effect in the position of the localized surface plasmon. A red shift of the extinction cross section with an increase of the disk size can be observed in Figure 2c. Indeed, the dependence of the spectral position of the plasmon peak with the disk size can be clearly traced from nanometric sizes up to micrometric ones. The geometrical morphology of PdH_x structures is thus responsible for the location of the LSPR of the PdH_x disks in the visible range of the spectrum, providing a unique opportunity for remote optical sensing of the H concentration in nanoscale disks.

In order to further clarify the effect of hydrogen uptake in the stoichiometric PdH_x nanodisks, we show in Figure 3 the

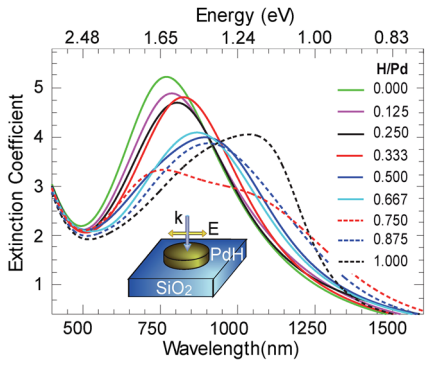

Figure 3. Extinction spectra of PdH_x disks of 20 nm thickness and 190 nm in diameter with uniform stoichiometry placed on a SiO_2 substrate evaluated for different x = H/Pd values. The disks are characterized by the dielectric functions as obtained from the TDDFT calculations in Figure 1b.

extinction cross section of PdH_x disks on a SiO_2 substrate as a function of the H/Pd ratio (H concentration) using the ab initio dielectric function obtained in Figure 1b. A 20 nm thick disk of diameter 190 nm is considered. The LSPR shift from 1.61 eV for pure Pd (green line) to 1.21 eV for $PdH_{x=1}$ (dashed black line) is conspicuous in Figure 3.

In reality, however, the PdH_x systems with $x > 0$ are not single-domain crystals but present a mixture of two phases called α and β. The α phase is characterized by a very small concentration of H atoms. Consequently, the dielectric properties of the α phase are very close to that of pure Pd. The β phase is characterized by an elevated concentration of H, and its dielectric properties can be approximated as those of PdH. One can thus try to understand the dielectric properties of PdH_x as being a mixture of two media, (i) an α phase (occupying $1 - f_\beta$ space) with $\omega_P^\alpha \approx 8$ eV and (ii) a β phase (occupying f_β space) with $\omega_P^\beta \approx 4.2$ eV. In a simple picture, the dielectric properties of such a composite system can be characterized by an effective dielectric function ε_{eff} defined through the loss function as

$$\varepsilon_{eff}^{-1} = (1 - f_\beta)\cdot\varepsilon_\alpha^{-1} + f_\beta\cdot\varepsilon_\beta^{-1} \quad (1)$$

The result of the loss function of this simple effective medium approach for different fractions of the β phase is presented in Figure 4a. Here, it can be clearly observed that, in a realistic PdH_x sample composed of α and β domains, the assumption of a linear downshift of ω_P with x breaks down. Increasing the concentration of H in PdH_x results in a gradual decrease of intensity of the pure Pd peak at ω_P^α, together with a gradual development of a fixed plasmon peak of the β phase at ω_P^β. This scenario was already discussed in ref 32 based on the experimental plasmonic spectra of bulk PdH_x systems. The measured evolution of the LSPR peak energy in PdH_x nanostructures then cannot be explained in terms of a simple linear downshift of the bulk plasmon energy ω_P shift when a simple admixture of phases in the bulk loss function is considered, as demonstrated in Figure 4a. Therefore, we proceed now to properly account for geometrical effects derived from the finite size of the Pd nanodisks as well as to adopt a more complete description of the phase distribution within the bulk response.

Recent experiments that explore this potential of plasmonics to sense the storage of H in metallic particles show that Pd metal gets saturated at fractions of H of about $x \approx 0.6$–0.7.[5,6] Therefore, two situations would, in principle, be possible in the diffusion of H in the Pd disks, (i) a homogeneous diffusion of H in Pd, with a constant concentration of H all over the Pd material, or (ii) an inhomogeneous distribution of two phases named α and β phases, consisting of domains of pure crystalline Pd and Pd–H, respectively, as is customary in bulk systems.[33,34]

dx.doi.org/10.1021/jz3007723 | J. Phys. Chem. Lett. 2012, 3, 2556–2561

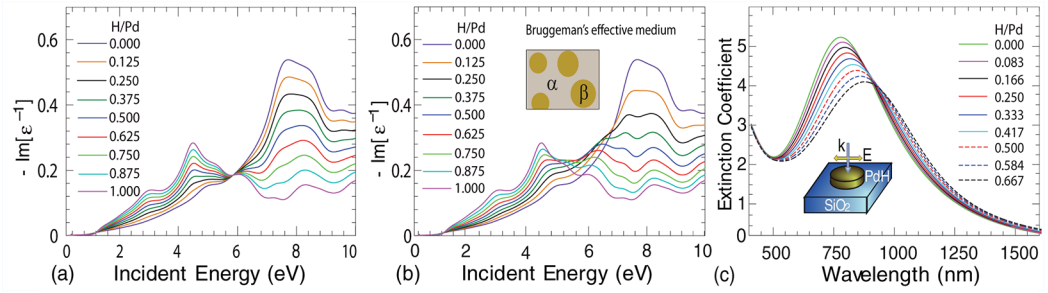

Figure 4. Evolution of bulk plasmon peaks of PdH_x with H uptake with use of a dielectric function derived from (a) a simple effective medium following eq 1 and (b) with use of Bruggeman's effective medium derived from eq 2 with the β phase assumed to be characterized by $PdH_{x=1}$. (c) Extinction spectra for a PdH_z disk of 20 nm thickness and 190 nm in diameter placed on a SiO_2 substrate calculated using Bruggeman's effective dielectric functions (eq 2) with a β phase domain characterized as $PdH_{x=0.667}$ for different z = H/Pd ratios of the entire system.

To discriminate between both situations, we adopt an effective medium approach to describe the optical response of the whole system composed of both phases. To construct the corresponding effective dielectric function, $\varepsilon_{\text{eff}}(z)$, (with z as the H/Pd number ratio in the entire effective medium), we take a weighted average of the ab initio calculated dielectric functions for Pd (taken here as a representee of the α phase) and for $PdH_{x=0.667}$ (β phase) following Bruggeman's effective medium approximation[35−37]

$$f_\beta \cdot \frac{\varepsilon_\beta - \varepsilon_{\text{eff}}(z)}{\varepsilon_\beta + 2\varepsilon_{\text{eff}}(z)} + (1 - f_\beta) \cdot \frac{\varepsilon_\alpha - \varepsilon_{\text{eff}}(z)}{\varepsilon_\alpha + 2\varepsilon_{\text{eff}}(z)} = 0 \quad (2)$$

where ε_α and ε_β are the dielectric functions of the α and β phases and f_β is the fraction of the saturated β phase. The dielectric loss function calculated for the Bruggeman's effective medium can be seen in Figure 4b. This effective dielectric function can be also used in the full calculation of the disk response as in Figures 2c and 3. Figure 4c shows the extinction spectra in the case of a disk of 190 nm diameter and 20 nm thickness on the SiO_2 substrate. A constant red shift of the LSPR of the entire two-phase system is observed as the H/Pd ratio increases, following the increase of the β phase presence f_β. We also calculate the extinction for a larger disk of diameter 300 nm, obtaining the same trend for the LSPR shift (not shown here).

To get more information about the domain distribution and H saturation in the Pd−H system, we test a different level of saturation for the β phase in eq 2 by setting x = 1 ($PdH_{x=1}$) in the dielectric function characterizing ε_β. The electrodynamical calculations are repeated using this modified effective dielectric function to obtain the disk response for increasing H concentration following an increase of the β phase presence f_β. In Figure 5, the calculated LSPR shift for this saturation (x = 1) in the case of a disk of 20 nm thickness and 300 nm in diameter (blue dots) is compared with the shift obtained with the original saturation adopted for the β phase ($PdH_{x=0.667}$, red dots) in the effective dielectric function. The LSPR shift for an homogeneous medium (black squares) and the experimentally observed shift from ref 6 (green dots) are also displayed for direct comparison.

Our theoretical calculations of the LSPR shift using a saturation value of x = 0.667 for the β phase (red dots) show excellent agreement with the measured experimental values of the shift, validating the assumption made for the admixture of the α and β phases. Furthermore, when the β phase is taken as fully saturated, $PdH_{x=1}$ (blue dots), a strong deviation of the behavior of the LSPR shift can be observed when compared

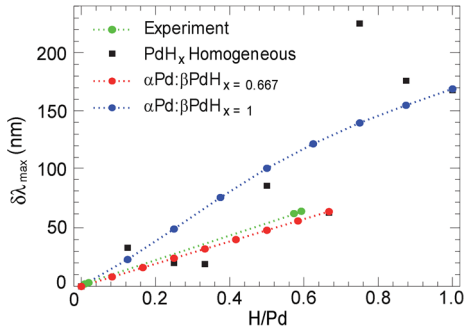

Figure 5. LSPR shifts calculated for a Pd−H disk of 20 nm thickness and 300 nm in diameter plotted as a function of the z = H/Pd ratio. The resonance shifts are calculated using Bruggeman's effective dielectric function (eq 2) with the β phase taken as $PdH_{x=0.667}$ (red dots) and as $PdH_{x=1}$ (blue dots). A comparison with experimental results from ref 6 (green dots) is shown.

with the experimental values and with the linear tendency obtained theoretically with use of $PdH_{x=0.667}$. This deviation seems to discard the possibility of full hydrogenation of the β phase domains in Pd−H nanostructures. The LSPR shift thus provides valuable information about the dynamics of domain formation in hydrogen uptake by the Pd nanodisks. However, this conclusion should be taken with caution as temperature and nanodisk boundaries[18] might influence the observations. Future investigations should take into account these and other possible effects.

Our results may look rather puzzling at first sight; we obtain a linear shift of the LSPR frequency in PdH_x systems when increasing x, without invoking any linear shift of the bulk plasmon energy ω_P. The reason for the linear shift, however, can be easily understood by analyzing the evolution of the dielectric loss function $-\text{Im}\{\varepsilon_{\text{eff}}^{-1}]\}$ derived from the Bruggemann's approximation as the H concentration x varies. This evolution is shown in Figure 4b for straight comparisson with the simple linear admixture of phases. Contrary to the evolution of the effective loss function in the simple approach in Figure 4a, the effective loss function that involves the more complex admixture of phases given by eq 2 varies gradually (almost linearly) with x in the energy interval of interest for plasmonic sensing (1−3 eV), this being the reason for the gradual shift of the plasmon response observed. Furthermore, if the excitation energy is tuned by modifying the system size, geometry, or environment, strong nonlinearities in the LSPR with H concentration would then appear. Slight differences between the simulations and the experimental results can be associated

dx.doi.org/10.1021/jz3007723 | J. Phys. Chem. Lett. 2012, 3, 2556−2561

with the large surface roughness caused by the hydrogenation of the Pd disks.[5]

In summary, by combining an ab initio description of the atomic-level properties of PdH_x with the full electrodynamical calculation of light scattering in nanoscale geometries, we have theoretically demonstrated that plasmonic sensing techniques are sensitive enough to be used as valuable tools for studying the dynamics of structural changes in metal hydride nanosystems. In the particular case of PdH_x nanodisks, the comparison of our theoretical results with recent experimental measurements validated quantitatively that H saturation takes place at $x \approx 0.667$ in the β phase. The methodology developed here will therefore bring further advance in the understanding of hydrogen absorption and diffusion in metal nanostructures.

AUTHOR INFORMATION

Corresponding Author

*E-mail: aizpurua@ehu.es.

Notes

The authors declare no competing financial interest.

ACKNOWLEDGMENTS

This work was supported in part by the Basque Departamento de Educación, Universidades e Investigación (Grant No. IT-366-07), the Spanish Ministerio de Ciencia e Innovación (Grant No. FIS2010-19609-C02-00), and the ETORTEK 2011 project nanoiker of the Dept. of Industry of the Basque government. We thank Prof. I. Zorić at Chalmers University of Technology for providing the experimental data in ref 6.

REFERENCES

(1) Maier, S. A. *Plasmonics: Fundamentals and Applications*; Springer: New York, 2007.

(2) Pelton, M.; Aizpurua, J.; Bryant, G. W. Metal-nanoparticle Plasmonics. *Laser Photon. Rev.* **2008**, *2*, 136−159.

(3) Anker, J. N.; Hall, W. P.; Lyandres, O.; Shah, N. C.; Zhao, J.; Van Duyne, R. P. Biosensing with Plasmonic Nanosensors. *Nat. Mater.* **2008**, *7*, 442−453.

(4) Liu, N.; Tang, M. L.; Hentschel, M.; Giessen, H.; Alivisatos, A. P. Nanoantenna-Enhanced Gas Sensing in a Single Tailored Nanofocus. *Nat. Mater.* **2011**, *10*, 631−636.

(5) Langhammer, C.; Zorić, I.; Kasemo, B.; Clemens, B. M. Hydrogen Storage in Pd Nanodisks Characterized with a Novel Nanoplasmonic Sensing Scheme. *Nano Lett.* **2007**, *7*, 3122−3127.

(6) Zorić, I.; Larsson, E. M.; Kasemo, B.; Langhammer, C. Localized Surface Plasmons Shed Light on Nanoscale Metal Hydrides. *Adv. Mater.* **2010**, *22*, 4628−4633.

(7) Tang, M. L.; Liu, N.; Dionne, J. A.; Alivisatos, A. P. Observations of Shape-Dependent Hydrogen Uptake Trajectories from Single Nanocrystals. *J. Am. Chem. Soc.* **2011**, *133*, 13220−13223.

(8) Tittl, A.; Kremers, C.; Dorfmüller, J.; Chigrin, D. N.; Giessen, H. Spectral Shifts in Optical Nanoantenna-Enhanced Hydrogen Sensors. *Opt. Mater. Express* **2012**, *2*, 111−118.

(9) Xie, B.; Liu, L.; Peng, X.; Zhang, Y.; Xu, Q.; Zheng, M.; Takiya, T.; Han, M. Optimizing Hydrogen Sensing Behavior by Controlling the Coverage in Pd Nanoparticle Films. *J. Phys. Chem. C* **2011**, *115*, 16161−16166.

(10) Wilde, M.; Fukutani, K.; Ludwig, W.; Brandt, B.; Fischer, J.-H.; Schauermann, S.; Freund, H.-J. Influence of Carbon Deposition on the Hydrogen Distribution in Pd Nanoparticles and Their Reactivity in Olefin Hydrogenation. *Angew. Chem., Int. Ed.* **2008**, *47*, 9289−9293.

(11) Tittl, A.; Mai, P.; Taubert, R.; Dregely, D.; Liu, N.; Giessen, H. Palladium-Based Plasmonic Perfect Absorber in the Visible Wavelength Range and Its Application to Hydrogen Sensing. *Nano Lett.* **2011**, *11*, 4366−4369.

(12) Schlapbach, L.; Zuttel, A. Hydrogen-Storage Materials for Mobile Applications. *Nature* **2001**, *414*, 353−358.

(13) Pundt, A.; Kirchheim, R. Hydrogen in Metals: Microstructural Aspects. *Annu. Rev. Mater.* **2006**, *36*, 555−608.

(14) Yamauchi, M.; Kobayashi, H.; Kitagawa, H. Hydrogen Storage Mediated by Pd and Pt Nanoparticles. *ChemPhysChem* **2009**, *10*, 2566−2576.

(15) Eberle, U.; Felderhoff, M.; Schulth, F. Chemical and Physical Solutions for Hydrogen Storage. *Angew. Chem., Int. Ed.* **2009**, *48*, 6608−6630.

(16) Berube, V.; Radtke, G.; Dresselhaus, M.; Chen, G. Size Effects on the Hydrogen Storage Properties of Nanostructured Metal Hydrides: A Review. *Int. J. Energy Res.* **2007**, *31*, 637−663.

(17) Langhammer, C.; Zhdanov, V. P.; Zorić, I.; Kasemo, B. Size-Dependent Kinetics of Hydriding and Dehydriding of Pd Nanoparticles. *Phys. Rev. Lett.* **2010**, *104*, 135502.

(18) Delogu, F. Smooth Size Effects in Pd and PdH_x Nanoparticles. *J. Phys. Chem. C* **2010**, *114*, 18085−18090.

(19) Langhammer, C.; Zhdanov, V. P.; Zorić, I.; Kasemo, B. Size-Dependent Hysteresis in the Formation and Decomposition of Hydride in Metal Nanoparticles. *Chem. Phys. Lett.* **2010**, *488*, 62−66.

(20) Silkin, V. M.; Chernov, I. P.; Koroteev, Y. M.; Chulkov, E. V. Low-Energy Collective Electronic Excitations in Pd Metal. *Phys. Rev. B* **2009**, *80*, 245114.

(21) Díez Muiño, R.; Sánchez-Portal, D.; Silkin, V. M.; Chulkov, E. V.; Echenique, P. M. Time-Dependent Electron Phenomena at Surfaces. *Proc. Natl. Acad. Sci. U.S.A.* **2011**, *108*, 971−976.

(22) García de Abajo, F. J.; Howie, A. Retarded Field Calculation of Electron Energy Loss in Inhomogeneous Dielectrics. *Phys. Rev. B.* **2002**, *65*, 115418.

(23) Langhammer, C.; Yuan, Z.; Zorić, I.; Kasemo, B. Plasmonic Properties of Supported Pt and Pd Nanostructures. *Nano Lett.* **2006**, *6*, 833−838.

(24) Silkin, V. M.; Díez Muiño, R.; Chernov, I. P.; Chulkov, E. V.; Echenique, P. M. Tuning the Plasmon Energy of Palladium Hydrogen Systems by Varying the Hydrogen Concentration. *J. Phys.: Condens. Matter* **2012**, *24*, 104021.

(25) Favier, F.; Walter, E. C.; Zach, M. P.; Benter, T.; Penner, R. M. Hydrogen Sensors and Switches from Electrodeposited Palladium Mesowire Arrays. *Science* **2001**, *293*, 2227−2231.

(26) Ingham, B.; Toney, M. F.; Hendy, S. C.; Cox, T.; Fong, D. D.; Eastman, J. A.; Fuoss, P. H.; Stevens, K. J.; Lassesson, A.; Brown, S. A.; Ryan, M. P. Particle Size Effect of Hydrogen-Induced Lattice Expansion of Palladium Nanoclusters. *Phys. Rev. B* **2008**, *78*, 245408.

(27) Wolf, R. J.; Lee, M. W.; Davis, R. C.; Fay, P. J.; Ray, J. R. Pressure-Composition Isotherms for Palladium Hydride. *Phys. Rev. B.* **1993**, *48*, 12415−12418.

(28) Silkin, V. M.; Chernov, I. P.; Echenique, P. M.; Koroteev, Y. M.; Chulkov, E. V. Influence of Hydrogen Absorption on Low-Energy Electronic Collective Excitations in Palladium. *Phys. Rev. B* **2007**, *76*, 245105.

(29) Schirber, J. E.; Morosin, B. Lattice Constants of β-PdH_x and β-PdD_x with x near 1.0. *Phys. Rev. B* **1975**, *12*, 117−118.

(30) Koroteev, Y. M.; Gimranova, O. V.; Chernov, I. P. Hydrogen Migration in Palladium: First-Principle Calculations. *Phys. Solid State* **2011**, *53*, 896−900.

(31) Aizpurua, J.; Hanarp, P.; Sutherland, D. S.; Käll, M.; Bryant, G. W.; García de Abajo, F. J. Optical Properties of Gold Nanorings. *Phys. Rev. Lett.* **2003**, *90*, 057401.

(32) Bennett, P. A.; Fuggle, J. C. Electronic Structure and Surface Kinetics of Palladium Hydride Studied with X-ray Photoelectron Spectroscopy and Electron-Energy-Loss Spectroscopy. *Phys. Rev. B* **1982**, *26*, 6030−6039.

(33) Wicke, E.; Blaurock, J. New Experiments on and Interpretations of Hysteresis Effects of Pd-D2 and Pd-H2. *J. Less Common Met.* **1987**, *130*, 351−363.

(34) Yamada, Y.; Tajima, K.; Bao, S.; Okada, M.; Yoshimura, K. Hydrogenation and Dehydrogenation Processes of Palladium Thin

Films Measured in situ by Spectroscopic Ellipsometry. *Sol. Energy Mater. Sol. Cells* **2009**, *93*, 2143−2147.
(35) Aspnes, D. E. Plasmonics and Effective-Medium Theories. *Thin Solid Films.* **2011**, *519*, 2571−2574.
(36) Ahn, J. S.; Kim, K. H.; Noh, T. W.; Riu, D.-H.; Boo, K.-H.; Kim, H.-E. Effective-Medium Theories for Spheroidal Particles Randomly Oriented on a Plane: Application to the Optical Properties of a SiC Whisker-Al_2O_3 Composite. *Phys. Rev. B* **1995**, *52*, 15244−15252.
(37) Garnett, J. C. M. Colours in Metal Glasses and in Metallic Films. *Phil. Trans. R. Soc. Lond. A* **1904**, *203*, 385−420.
(38) Netzer, F. P.; El Gomati, M. M. Electronic Excitations on Clean and Adsorbate Covered Pd(111) by Angle Resolved Electron Energy Loss Spectroscopy. *Surf. Sci.* **1983**, *124*, 26−38.
(39) Bornemann, T.; Eickmans, J.; Otto, A. Interaction of d-Electron Excitations and Plasmons in Pd, Ag, Cd, In, Sn and Sb. *Solid State Commun.* **1988**, *65*, 381−384.
(40) Hagelin, H. A. E.; Weaver, J. F.; Hoflund, G. B.; Salaita, G. N. Electron Energy Loss Spectroscopic Investigation of Palladium Metal and Palladium(II) Oxide. *J. Electron Spectrosc. Relat. Phenom.* **2002**, *124*, 1−14.
(41) Weaver, J. H. Optical Properties of Rh, Pd, Ir, and Pt. *Phys. Rev. B* **1975**, *11*, 1416−1425.
(42) Palik, E. D. *Handbook of Optical Constants of Solids*; Academic Press: San Diego, CA, 1991.
(43) Maksimov, E. G.; Mazin, I. I.; Rashkeev, S. N.; Uspenski, Y. A. First-Principles Calculations of the Optical Properties of Metals. *J. Phys. F: Met. Phys.* **1988**, *18*, 833−849.
(44) Fehrenbach, G.-M. Theoretical Prediction of the Peak Structure in the EELS Spectrum of Palladium. *Phys. Rev. B* **1999**, *59*, 15085−15092.
(45) Krasovskii, E. E.; Schattke, W. Semirelativistic Technique for **k**·**p** Calculations: Optical Properties of Pd and Pt. *Phys. Rev. B* **2001**, *63*, 235112.
(46) Keast, V. J. Ab initio Calculations of Plasmons and Interband Transitions in the Low-Loss Electron Energy-Loss Spectrum. *J. Electron Spectrosc. Relat. Phenom.* **2005**, *143*, 97−104.